

THE AC IMPEDANCE OF FROG SKIN AND ITS RELATION TO ACTIVE TRANSPORT

A. C. BROWN *and* K. G. KASTELLA

*From the Departments of Physiology and Biophysics and of Electrical Engineering,
University of Washington, Seattle*

ABSTRACT The AC electrical impedance of frog skin was measured in the range 1 cycle/second to 50 kc/second by injecting current sinusoidally at low current density. The behavior of the skin was found to be linear so the usual concepts of impedance could be validly employed. In the range 1 cycle/second to 5 kc/second, the impedance traces out a circular arc locus with its center off the real axis; thus the skin could be represented by a series resistance and a parallel combination of a conductance and a phase shift element. The phase shift element has an impedance angle of about 80°, current leading voltage, with an equivalent capacitance of about 2 $\mu\text{f}/\text{cm}^2$. The phase shift and the equivalent capacitance were independent of the experimental conditions. The parallel conductance, which was responsible for most of the low frequency impedance, could be subdivided into two approximately equal conductances, one associated with sodium ion current and the other associated with chloride ion current. Both currents were determined mainly by the concentrations of the respective ions bathing the outside of the skin. The response to changes in concentration and the response to CO₂ indicated that the chloride current was passive, but the sodium current appeared to be associated with the active transport mechanism; little sodium could pass through the skin unless associated with active transport.

INTRODUCTION

The skin of the frog and the toad has been widely and productively employed in the investigation of active ion transport. In particular, the measurements of the electric potential and the electric current associated with the movement of charged particles have proven to be valuable indices of active transport. The two commonly measured parameters are the DC or steady-state open circuit potential and short circuit current developed by the skin (Ussing and Zerahn, 1951; Ussing, 1960).

The AC impedance of biological tissue to sinusoidal voltage changes also has been widely examined usually for the purpose of developing an equivalent circuit for the passive spread of electric current, as, for example, in the striated muscle fiber (Falk and Fatt, 1964, and Fatt, 1964), in the nerve axon (Cole and Curtis, 1936), or the current pathways in the cerebral cortex (Ranck, 1963*a* and 1963*b*; see also Schwan, 1957).

The object of this work is to combine these two avenues of study by developing, from the AC impedance measured under various circumstances, an equivalent circuit for frog skin, and then evaluating the role of the elements of this circuit in active transport.

METHODS

Procedure. Frogs, species *Rana pipiens*, were pithed, the abdominal skin rapidly excised, rinsed in a modified Ringer's solution, and clamped in a special chamber. Perfusion was begun immediately with modified Ringer's "normal" solution (the composition of solutions is given below). To measure the electrical potential across the skin, KCl-agar electrodes were inserted into the chamber until they almost touched the skin. When appropriate, current was passed through the skin by means of saturated NaCl-agar salt bridges and Ag-AgCl electrodes introduced at ends of the chamber (see Fig. 1). The procedure is similar to that described by Ussing and Zerahn (1951).

After the initial mounting of the skin, its open circuit (no current injected) DC voltage, V_{oc} , was monitored until it reached a steady level, generally in the range 30 to 60 mv inside positive. (Skins with voltages of less than 30 mv were rejected). In some experiments, DC short circuit current (the injected current necessary to bring the skin potential to zero) was measured, as an index of active sodium transport; it averaged $26 \mu\text{amp}/\text{cm}^2$.

When V_{oc} attained a steady level, the sine wave oscillator was switched into the circuit, its output adjusted to deliver 7 to $10 \mu\text{amp}/\text{cm}^2$ peak to peak through the skin; then the data were recorded, the oscillator switched out, and another frequency selected. Each test run began at 1 cycles/second and progressed to at least 50 kc/second in about ten steps. To assure that no systematic changes occurred during the series, V_{oc} was checked between every second or third frequency change; also, following the 50 kc/second step, measurements at three of the lower frequencies were repeated. Then a new test solution was introduced into the chamber, V_{oc} was monitored until steady, and a similar series of sine waves tests was carried out.

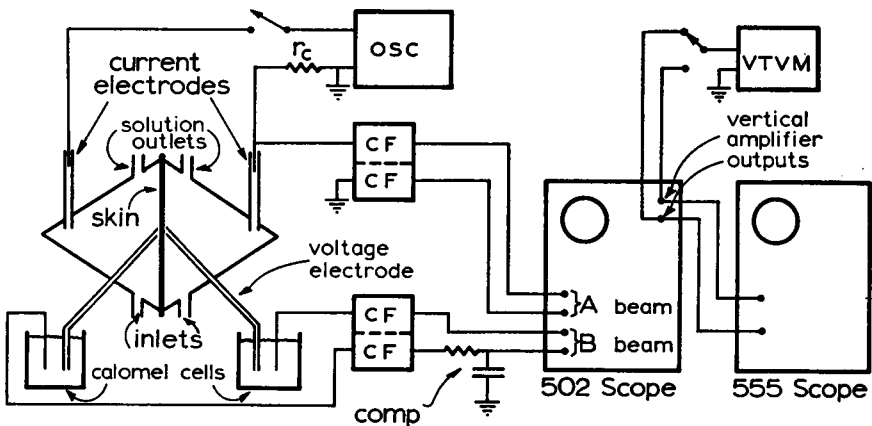


FIGURE 1 The experimental arrangement for the impedance measurements. Cathode followers are noted by "CF"; two pairs were used. The RC compensation network used to increase the common mode rejection is indicated by "comp."

Electrical Measurements. The voltage electrodes, which were saturated KCl-agar salt bridges, were led to saturated calomel half-cells. The output of the calomel cells was fed into DC coupled cathode followers, used to provide a high input impedance. These were followed by an RC (resistance-capacitance) trimming network, which had been adjusted to maximize the common mode rejection. Next, the skin voltage signal was led into the differential input of one channel of a Tektronix 502 dual beam oscilloscope (Tektronix, Inc., Portland, Oregon).

Current was injected using a sine wave oscillator (Hathaway N-2, Hathaway Instruments, Denver, Colorado) connected to the current electrodes in series with a known resistor, r_c . The voltage drop across the resistor, recorded on the other channel of the oscilloscope, was used to calculate the current through the skin. The value of r_c was adjusted to permit the use of the same sensitivity setting on both channels of the Tektronix 502, since at the higher frequencies the two vertical amplifiers had similar frequency response and phase shift characteristics only if their gains (or sensitivities) were the same.

In the first few experiments the impedance was calculated from photographs of the current and voltage traces. In later experiments, the outputs of the vertical amplifiers of the Tektronix 502 were brought out; the magnitude of the impedance was calculated from the ratio of the voltage and current amplitudes using a VTVM (vacuum tube voltmeter) connected to the vertical outputs and the phase angle was measured by feeding these signals into a second dual beam oscilloscope (Tektronix 555) in which one time base was delayed by a known amount until the two traces superimposed. The accuracy of the impedance measurement was about 5 per cent for magnitude and 4° for phase at low and intermediate frequencies.

At higher frequencies, the accuracy was progressively decreased due to the combined effects of the reduction in the common mode rejection of the measuring system and relatively low impedance of the skin at these frequencies; the former led to increased response to the common mode signal while the latter led to smaller differential (or "true membrane") potential at the voltage electrodes. These frequency-dependent limitations were evaluated in the following ways:

(a) A dummy network was constructed with fixed resistors in place of the electrodes and the skin (*c.f.* Fig. 2); the simulated skin impedance was then calculated using the remainder of the measuring systems and compared with the known value. (b) A passive membrane of the type used for dialysis was substituted for the skin, and its impedance was measured in the same manner. The membrane was sufficiently thick to produce a low capacitance, but was freely permeable to sodium and chloride ions. Thus, the passive

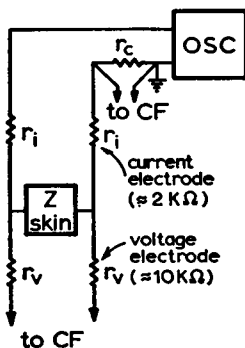


FIGURE 2 The electrical circuit used to simulate the electrodes and skin. The electrodes were replaced by fixed resistors and the skin was replaced by a known impedance.

membrane would be expected to present a constant and real (resistive) impedance to the flow of AC current; this expectation was compared with the actual measurements.

From these tests, it was concluded that the low and intermediate frequency accuracy extended to about 30 kc/second and that measurements were valid up to 50 kc/second but at reduced accuracy (impedance magnitude, ± 20 per cent; impedance angle, $+15^\circ$).

Solutions. The "normal" solution used in the initial perfusion was a modified Ringer's with the following concentrations: NaCl, 100 mM; KCl, 2 mM; CaCl₂, 2 mM; MgCl₂, 1.2 mM; KH₂PO₄, 0.02 mM; K₂HPO₄, 0.08 mM; glucose, 2 gm/liter; and was saturated with 100 per cent O₂. The "choline" solution was the same, except choline chloride, 100 mM, was substituted for NaCl; similarly, "isethionate" solution deviated from the normal solution only in the substitution of sodium isethionate, 100 mM, for the NaCl. Solutions of graded concentration of Na or Cl were made by combining the above; for example, the "10 per cent Na" solution contained 10 per cent (by volume) of the "normal" solution and 90 per cent of the "choline" solution, resulting in a sodium concentration of 10 mM. To suppress active transport, some solutions were saturated with oxygen containing 5 or 10 per cent CO₂ instead of pure oxygen.

RESULTS AND DISCUSSION

Linearity. The usual concepts associated with linear impedance can be validly employed only for linear circuits. To test for linearity, current was injected in the form of a sine wave and the voltage wave form was checked for harmonic distortion. No distortion was noted, a characteristic of a linear circuit. Also, the calculated impedance did not depend upon the amplitude of the injected current wave, up to 10 μ amp/cm² (the highest current density employed). Two limitations on these observations are, first that at 1 cycle/second (the lowest frequency used) it was difficult to inject current sinusoidally, due to a combination of electrode polarization and oscillator distortion; and second, at the highest frequencies (above 20 kc/second) the harmonics (if present) would be attenuated relative to the fundamental due to the limited frequency response of the system. Thus, at least within the limits of 1 cycle/second to 20 kc/second and at the low current densities used here, frog skin presents a linear impedance to electric current.

Impedance Plot. Since the circuit is linear, the ratio of voltage to current at a particular sine wave frequency can be plotted as a point on the complex plane; a typical plot of these values for various frequencies is shown in Fig. 3; note that the reactance axis is inverted so that negative reactance is upward.¹ All points were in the first quadrant, indicating that the current always leads the voltage but by less than 90° (with occasional exceptions at the highest frequencies).

The shape of the plot was the same for all skins, independent of experimental

¹ This inverted orientation of the reactance axis in impedance plots is at variance with normal practice in the electrical engineering and physics literature; however, it is the common convention in biology and physical chemistry and is employed here. Thus in this paper, a point in the first quadrant means resistive component of the impedance positive and reactive component negative; second quadrant, resistance and reactance both negative; third quadrant, resistance negative and reactance positive; fourth quadrant, resistance and reactance both positive.

conditions. At low frequency, the impedance was almost purely resistive, 900 to 7000 ohm-cm² in magnitude. As the frequency was increased, the impedance traced out a circular arc, again approaching a pure resistance of 50 to 300 ohm-cm² at about 5 kc/second; the center of the circle was depressed below the real axis. This part of the curve will be called the *circular locus*. Beginning at about 5 kc/second, the magnitude of the reactive component progressively increased as the frequency was raised, tracing out what will be termed the *high frequency locus*.

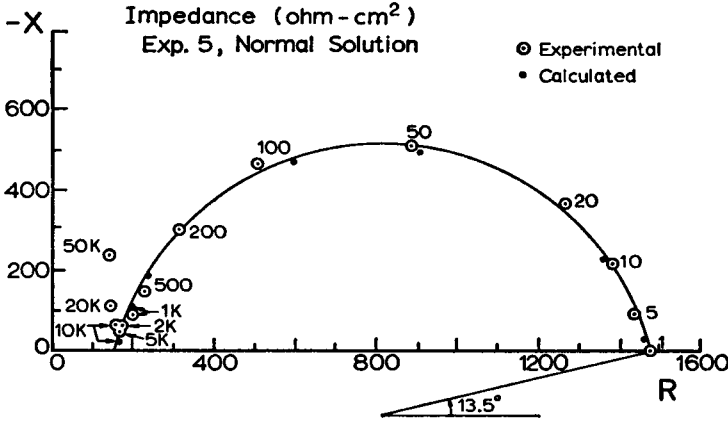


FIGURE 3 The impedance plot from a typical experiment, normal solution on both sides. The experimental points are noted by \odot ; the frequencies (in cycles/second) at which they were obtained are written alongside. The theoretical values calculated from equation (1) for the frequencies 1, 10, 50, 100, 500 cps, 1, and 10 kcps are indicated by \bullet .

It is difficult to characterize the high frequency locus. Its shape was variable, sometimes rising parallel to the imaginary axis, sometimes crossing into the second quadrant, and on one occasion crossing into the fourth quadrant. Also, the instrumentation was least reliable at the high frequency end of the range. Nevertheless, the general shape of the high frequency locus is considered accurate; it has been noted in other tissue (Ranck, 1963a), but its interpretation here is not clear.

Circular Locus. The circular impedance locus, which is characteristic of most biological materials and many physical dielectrics as well (Schwan, 1957; Smyth, 1955), will be considered in the remainder of this paper. Such a locus can be characterized by four constants illustrated in Fig. 4: R_0 , the intercept of the low frequency end of the arc with the real axis; R_∞ , the intercept of the high frequency end of the circular arc with the real axis; ϕ , the angle between the horizontal and the line from the center of the arc to R_0 ; and f_0 , the frequency of maximum reactance.

It can be shown that such a circular impedance locus can be described by the equation

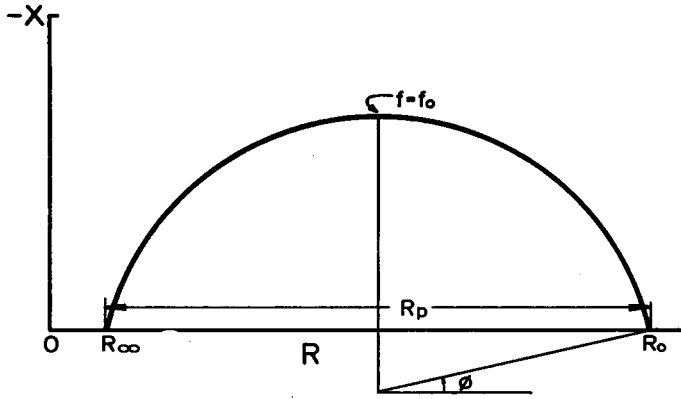


FIGURE 4 A schematic of the circular locus indicating how R_o , R_∞ , ϕ , f_o , and $R_p (= 1/g_p)$ are evaluated.

$$Z = R_\infty + \frac{R_o - R_\infty}{1 + (j\omega\tau)^{1-\alpha}} \quad (1)$$

where

$$\omega = 2\pi f$$

and

$$\alpha = \phi/90^\circ$$

The time constant, τ , can be evaluated by noting that the reactive component of equation (1) is maximum when $\omega\tau = 1$. Thus

$$\tau = \frac{1}{2\pi f_o} \quad (2)$$

where f_o is the frequency of maximum reactance.

The values of R_∞ , R_o , ϕ , and f_o for each experimental run are given in Table I.

It should be noted that any function of frequency of the form $j^{1-\alpha} f(\omega)$ could be substituted for the term $(j\omega\tau)^{1-\alpha}$ in equation (1) and still result in a circular arc with a depressed center, as long as $f(\omega)$ is a strictly monotonically increasing function of ω and $f(0) = 0$. To test whether equation (1) gives the correct dependence upon frequency as well as the correct shape, Z was calculated and compared with the experimental results. As can be seen from Fig. 3, the calculated and measured values are in good agreement.

Equivalent Circuit. An equivalent circuit which would give equation (1) is shown in Fig. 5; it consists of a resistance of value R_∞ in series with the parallel combination of a resistor R_p (of conductance g_p) and another impedance Z' , where

TABLE I
ELECTRICAL CONSTANTS FOR EACH EXPERIMENT

Exp. no.	Solution	R_{∞}	R_0	g_p	ϕ	f_0	C'	V_{00}
		<i>ohm-cm²</i>	<i>ohm-cm²</i>	<i>mmho/cm²</i>	<i>degrees cycle/second</i>	<i>μf/cm²</i>	<i>mv</i>	
1	Normal (both)	160	1100	1060	10.0	80	2.1	47-43
2	Normal (both)	190	890	1415	12.5	100	2.2	48-44
3	Normal (both)	130	1300	850	12.5	70	1.9	56-53
	Choline (both)	170	2650	400	12.0	30	2.1	4- 0
4	Normal (both)	140	930	1275	12.5	70	2.9	50-46
	Choline (both)	220	2670	410	6.5	20	3.2	2-(-1)
5	Normal (both)	160	1480	755	13.5	60	2.0	49-40
	Normal + 5% CO ₂	160	4460	230	9.0	18	2.0	8- 6
6	Normal (both)	160	3230	325	4.0	20	2.6	33-32
	Normal + 5% CO ₂	190	5150	200	7.5	15	2.1	2- 0
7	Normal (both)	130	2780	375	7.5	25	2.4	51-40
	Isethionate (both)	190	4840	215	4.0	14	2.4	50-44
	Choline (both)	220	6190	165	6.5	14	1.9	5- 1
8	Normal (both)	160	1810	605	21.0	34	2.8	48-44
	Isethionate (both)	280	3270	335	12.0	18	3.0	64-53
	Choline (both)	240	3300	325	12.0	20	2.6	10- 7
9	Normal (both)	190	820	1590	8.0	80	3.2	38-36
	Isethionate (both)	250	1880	610	13.0	38	2.6	39-32
	Isethionate + 10% CO ₂	280	3170	345	12.0	39	1.4	11- 8
10	Normal (both)	50	2450	415	8-0	24	2.8	42-40
	Isethionate + 10% CO ₂	90	3670	280	15.0	38	1.2	15-13
	Normal + 10% CO ₂	50	3420	295	13.0	38	1.2	9- 5
11	Normal (both)	130	3170	330	9.5	29	1.8	40-32
	Choline (out)	140	4870	210	8.0	20	1.7	12- 7
	Choline (both)	190	5280	195	7.0	13	2.4	5- 6
	Choline (in)	130	4080	250	9.0	24	1.7	19-14
	Normal (both)	140	3740	275	8.0	30	1.5	7-10
12	Normal (both)	90	1630	650	9.0	43	2.4	57-57
	Choline (out)	110	3170	325	6.0	30	1.7	10- 7
	1% Na (out)	110	2500	420	12.5	32	2.1	21-18
	3% Na (out)	90	1700	625	11.0	43	2.3	34-32
	10% Na (out)	80	1400	755	21.0	50	2.4	46-45
	30% Na (out)	90	1320	815	14.0	56	2.3	59-52
	Normal (both)	90	1630	650	6.0	44	2.3	52-50
13	Normal (both)	160	2670	400	6.0	30	2.1	57-44
	Isethionate (out)	170	5810	175	5.0	10	2.8	22-21
	Isethionate (both)	220	6970	150	5.5	9	2.6	18-18
	Isethionate (in)	220	4550	230	8.0	19	1.9	29-22
	Normal (both)	130	3710	280	6.0	26	1.7	36-33
14	Normal (both)	140	2010	535	8.5	35	2.4	44-32
	Isethionate (out)	130	3080	340	6.0	29	1.9	38-40
	Choline (out)	130	4460	230	6.5	21	1.7	6- 5

TABLE I (continued)

Exp. no.	Solution	R_{∞}	R_0	g_p	ϕ	f_0	C'	V_{00}
		ohm-cm ²	ohm-cm ²	mmho/cm ²	degrees	cycle/second	μf/cm ²	mv
15	Normal (both)	90	2060	510	11.0	35	2.3	63-61
	Isethionate (out)	130	3220	325	8.5	28	1.8	58-59
	1% Cl (out)	130	3250	320	7.0	29	1.7	60-60
	3% Cl (out)	110	3280	315	7.0	29	1.7	61-61
	10% Cl (out)	110	3280	315	8.0	28	1.8	59-59
	30% Cl (out)	130	3200	325	9.0	28	1.8	57-54
	Normal (both)	110	2540	410	9.5	32	2.0	59-55
16	Normal (both)	140	2030	530	11.5	38	2.2	34-31
	Choline (in)	140	2120	505	14.5	36	2.2	33-35
	1% Na (in)	160	2150	500	13.5	38	2.1	34-26
	3% Na (in)	170	2560	420	11.5	33	2.0	23-20
	10% Na (in)	160	2570	415	13.0	36	1.8	18-17
	Normal (both)	140	2685	390	15.0	35	1.8	15-16
17	Normal (both)	140	1870	580	12.0	30	3.1	66-56
	Isethionate (in)	190	1960	565	8.0	30	3.0	52-43
	1% Cl (in)	190	2790	385	7.5	19	3.2	46-38
	3% Cl (in)	190	2900	365	6.0	18	3.2	34-33
	10% Cl (in)	200	3440	310	9.0	16	3.1	35-32
	30% Cl (in)	170	3530	295	8.0	16	3.0	36-36
	Normal (both)	160	3610	290	8.0	15	3.1	46-44

"Both" indicates that the solution was used on both sides of the skin; "in" indicates that the solution was used on the inside only with normal on the outside; "out" indicates that the solution was used on the outside only with normal on the inside.

$$g_p = \frac{1}{R_p} = \frac{1}{R_0 - R_{\infty}}$$

and

$$Z' = R_p(j\omega\tau)^{\alpha-1} \tag{3}$$

The Phase Shift Element. Current through the element Z' leads the voltage by a constant angle of $(1-\alpha) \times 90^\circ$, while the magnitude of Z' decreases with increasing frequency in proportion to $1/\omega^{(1-\alpha)}$. If α were equal to zero, this element would be a pure capacitor of value C' where

$$C' = \tau g_p \tag{4}$$

The deviation of α from zero is a measure of how far this element departs from an ideal capacitor. The fact that α is not zero is responsible for the depressed center of the circular locus.

Dielectric relaxation is the mechanism most commonly postulated which can produce a constant phase shift (in other than multiples of 90°). This phenomenon

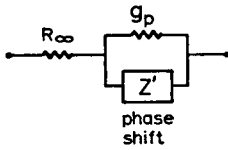


FIGURE 5 An equivalent circuit for the skin.

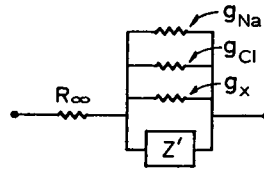


FIGURE 6 The skin equivalent circuit with g_p divided into its component conductances.

occurs when the displacement vector within the dielectric lags the electric field vector due to the inability of the dielectric polarization to follow rapid changes in the electric field. In the simplest case, this lag is characterized by a first order differential equation with a single time constant; the more general case, with an appropriate distribution of time constants, is necessary to explain the results seen here (Schwan, 1957). Alternatively, a constant phase-shift network can be synthesized from a capacitor paralleled by an infinite sequence of RC series elements (Schwan, 1957). A sheet of relatively closely packed cells, such as the stratum germinativum, could provide the proper physical configuration for such a circuit.

Whatever mechanism is responsible for the frequency independence of the phase shift, it does not seem to be associated with the conduction of ions, as noted in Table I. The angle ϕ does not depend upon the composition of the perfusion solution; it is not altered appreciably by suppression of active transport with CO_2 ; and it is relatively constant from skin to skin (in the same circumstances the magnitude of the impedance varies frequently by a factor of four or more). The mean value of ϕ was 9.7° , implying that current led voltage by about 80° through this element; the standard deviation of the phase shift of Z' in all circumstances from all skins was only 3.5° .

Finally, by assuming a parallel plate capacitor, an approximation to the physical dimensions of this capacitive element can be calculated from the equation

$$d = k\epsilon_0 A/C' \quad (5)$$

where d is the distance between the plates, k is the dielectric constant, ϵ_0 is the permittivity of free space, A is the area of the plates, and C' is the capacitance. The mean value of C'/A calculated from equation (4) is $2.24 \mu\text{f}/\text{cm}^2$, with standard deviation of $0.48 \mu\text{f}/\text{cm}^2$; the value of C' showed no systematic variation with solution composition or active transport suppression. Substituting in equation (5) gives the separation (in Angstrom units)

$$d = 3.9k$$

An exact estimate of the separation cannot be expected from this calculation because

of uncertainty in the value of k (which might range from 5, characteristic of lipids, to 80 for water) and because of possible folding or corrugation of this layer which would lead to a larger value of A than used in evaluating equation (5); also, the phase-shift element is not a pure capacitor. However, from the order of magnitude of d , the dielectric layer is probably no thicker than a single cell membrane.

Conductance of Sodium and Chloride. The results of the complete substitution of choline ion for sodium can be seen from several of the experiments listed in Table I, for example Experiment 3. As previously noted, there is no significant change in ϕ or in C' . However, there is a quite marked increase in R_o and a smaller but significant increase in R_∞ . The open circuit DC voltage decreased to about zero, an effect which may be attributed to the specificity of the active transport mechanism for sodium (Ussing and Zerahn, 1951).

Substitution of isethionate for chloride (*e.g.*, Experiment 7) leads to a similar pattern—namely a large increase in R_o , a smaller increase in R_∞ , and little systematic change in C' and ϕ —except that the DC voltage did not decrease, but frequently increased, possibly because of the inability of isethionate to mimic chloride ion in partially “short circuiting” the skin.

The interpretation of these results is based on the assumption that the region of the skin which comprises g_p is impermeable to both choline and isethionate; in other words, these ions cannot substitute for sodium and chloride in carrying current through g_p . Thus, any change seen when choline replaces sodium presumably is due only to the reduction of sodium concentration, rather than to any specific effect of choline; a similar relation is assumed between isethionate and chloride.

From the decrease in g_p seen on substitution of choline or isethionate, it is clear that both sodium and chloride are significant in determining this conductance. In terms of an equivalent circuit, g_p can be represented as the sum of three parallel conductances: g_{Na} , the conductance attributed to sodium; g_{Cl} , the conductance attributed to chloride; and g_s , the conductance attributed to all other ions present (see Fig. 6). Thus, using the assumptions about the conductivity of choline and isethionate, we may write

$$g_p(n) = g_{Na} + g_{Cl} + g_s \quad (6a)$$

$$g_p(ch) = g_{Cl} + g_s \quad (6b)$$

$$g_p(is) = g_{Na} + g_s \quad (6c)$$

where $g_p(n)$, $g_p(ch)$, and $g_p(is)$ indicate the parallel conductance when the skin is perfused on both sides with the normal solution, the choline substitute solution, or the isethionate substituted solution, respectively. The fraction (F) of the total current carried through g_p by sodium and chloride when the skin is exposed to the normal solution can be computed from

$$F_{Na} = \frac{g_{Na}}{g_p(n)} = \frac{g_p(n) - g_p(ch)}{g_p(n)} \quad (7a)$$

and

$$F_{Cl} = \frac{g_{Cl}}{g_p(n)} = \frac{g_p(n) - g_p(is)}{g_p(n)} \quad (7b)$$

The values of F_{Na} and F_{Cl} calculated from those experiments in which the sodium and/or the chloride were completely replaced are listed in Table II.

From the mean values of F_{Na} and F_{Cl} , it is clear that sodium and chloride each carry about half the current in g_p . Thus the current carried by other ions is quite low,

TABLE II
FRACTIONAL CONDUCTANCE OF g_p

Exp. no.	F_{Na}	$F_{Na}(in)$	$F_{Na}(out)$	F_{Cl}	$F_{Cl}(in)$	$F_{Cl}(out)$	F_{Co_2}
3	0.53	—	—	—	—	—	—
4	0.68	—	—	—	—	—	—
5	—	—	—	—	—	—	0.68
6	—	—	—	—	—	—	0.38
7	0.56	—	—	0.43	—	—	—
8	0.46	—	—	0.45	—	—	—
9	—	—	—	0.62	—	—	0.17
10	—	—	—	—	—	—	0.29
11	0.35	0.13	0.33	—	—	—	—
12	0.50	—	—	—	—	—	—
13	—	—	—	0.56	0.25	0.52	—
14	—	—	0.57	—	—	0.37	—
15	—	—	—	—	—	0.34	—
16	—	0.00	—	—	—	—	—
17	—	—	—	—	0.02	—	—
Mean	0.51	0.06	0.45	0.51	0.13	0.41	0.38

and g_o must be a relatively small fraction of $g_p(n)$. The assumption that choline and isethionate do not contribute to g_p is confirmed by the observation that the sum of F_{Na} and F_{Cl} is approximately unity.

The low value of R_∞ (compared to R_p) indicates that Na^+ and Cl^- were not greatly impeded in moving through the tissue which comprised this resistance. The value of R_∞ increased somewhat upon substitution of choline or isethionate, but proportionally less than the increase in R_p . This implies that isethionate and choline can carry current through this tissue, although at a lower rate than sodium and chloride.

Source of Conducted Ions. Ions responsible for the parallel conductance, g_p , might have come from solutions bathing both sides of the skin, or could have been supplied mainly from one side. To decide between these alternatives, sodium

or chloride was removed from one side at a time by substituting choline or isethionate in the perfusing solution and g_p was determined. This procedure necessitated a number of solution changes and hence took several hours; as a result the measurements for the first and last run frequently differed, although the experimental conditions were the same. To compensate for this drift, it was assumed that the conductance, g_p , changed linearly with run, permitting calculation of the fractional conductances as shown in Fig. 7.

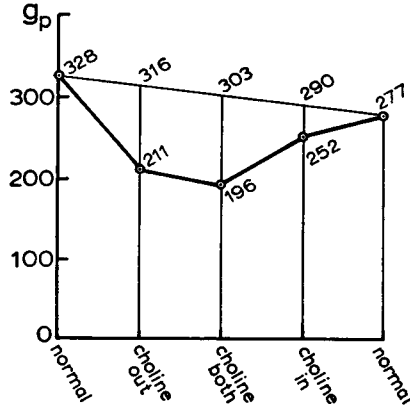


FIGURE 7 Compensation for conductance drift. The parallel conductance with normal solution was not usually constant but tended to decrease with time, as illustrated by the first and last runs in this figure. To obtain a value for $g_p(n)$ to be used in the calculation for the fractional conductances F , it was assumed that $g_p(n)$ changed linearly with run. For example, $g_p(n)$ for the middle run is taken as half way between the initial and final values, giving $F_{Cl} = (303 - 196)/(303) = 0.35$. The time interval between runs is approximately the same.

The results of these experiments are listed in Table II. The effect on conductance was measured in terms of the fractional decrease in g_p in a manner similar to equations (7); for example:

$$F_{Na}(in) = \frac{g_p(n) - g_p(\text{choline inside})}{g_p(n)}$$

Other fractional conductances were similarly defined.

These data show that the ions which determine both g_{Na} and g_{Cl} come predominantly from the outside solution.

Effect of Concentration. The influence of sodium and chloride concentration on the parallel conductance, g_p , was examined by replacing these ions in graded steps with choline and isethionate. The sequence normally used was 100, 0, 1, 3, 10, 30, and 100 meq/liter of Na^+ or Cl^- . As in the preceding section, the drift of skin conductance with time was corrected when necessary.

The resulting plot of fractional conductance as a function of concentration is

given by Fig. 8. The contribution of chloride to g_p is seen to increase linearly with chloride concentration. In contrast, the sodium conductance increases rapidly at low sodium concentrations, reaching a peak and perhaps decreasing slightly at higher concentrations.

The dependence of g_{Cl} upon $[Cl^-]$ needs no special explanation since it is similar to the behavior of chloride ion in a dilute free solution: that is, the current carried by chloride is directly proportional to the chloride concentration (Moore, 1955).

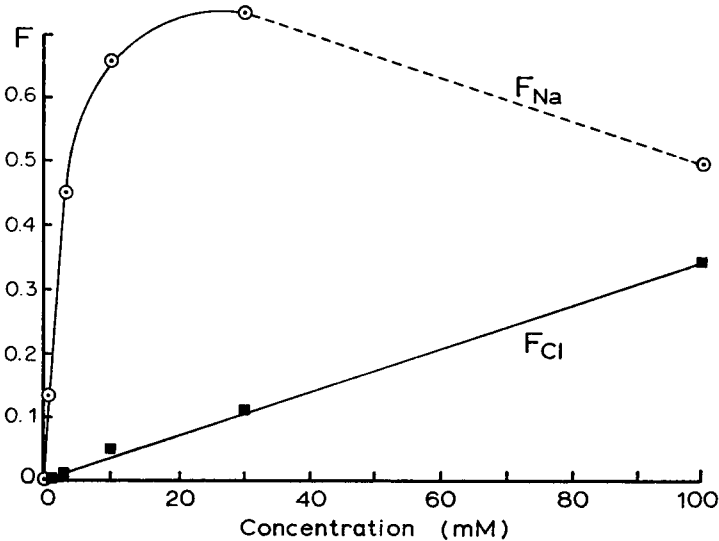


FIGURE 8 The fractional conductances for sodium and chloride calculated as a function of the concentration of the respective ion on the outside of the skin (Experiments 12 and 15).

The sodium curve is less easily explained. The most likely hypothesis is that g_{Na} reflects the active transport kinetics of sodium through the skin. Supporting this interpretation are the following: (a) The saturation at low concentrations seen here is typical of active transport. (b) This curve is quite similar to that of sodium flux as a function of sodium concentration in the short circuited frog skin (Kirschner, 1955). (c) This curve is similar to the dependence of short circuit current upon sodium concentration (Brown, 1962). (d) Calculations based on a kinetic model of active sodium transport have given results similar to our data (Snell and Leeman, 1957).

Effect of CO_2 . The above discussion of g_{Na} implies that the AC sodium current is not conducted by a pathway parallel to active transport; that is, there appears to be only one main pathway for sodium through the skin, that pathway which is also responsible for active transport. To test this hypothesis further, g_p was measured with active transport suppressed by saturating the perfusing solutions with

5 or 10 per cent CO₂ (Ussing and Zerahn, 1951) while maintaining the normal amount of sodium. The use of CO₂ was considered preferable to a metabolic poison such as cyanide or dinitrophenol, since these latter may have undesirable or unknown side effects. The drop in DC open circuit voltage indicates that the CO₂ concentration used effectively suppressed the active transport.

The magnitude of this effect is indicated by F_{CO_2} , the fraction by which g_p is reduced due to the introduction of CO₂, and is calculated from

$$F_{CO_2} = \frac{g_p(O_2) - g_p(CO_2)}{g_p(O_2)} \quad (8)$$

where $g_p(O_2)$ is the parallel conductance with 100 per cent oxygen, and $g_p(CO_2)$ is the parallel conductance with CO₂ present. The results are shown in Table II.

From this table it can be seen that the drop in conductance associated with suppression of active transport is of the same order of magnitude as the conductance decrease upon withdrawal of sodium. This depression occurs even with the isethionate solution (Experiment 10) indicating that changes in chloride conductance could not be responsible for this result. These observations confirm the previous assumption that if sodium is not conducted by the active transport pathway it cannot pass through the skin or move back and forth within the skin. The fact that F_{CO_2} was generally less than F_{Na} may be due to incomplete inhibition of the active transport mechanism by the CO₂ concentration used here, an explanation supported by the failure of V_{oo} to be depressed completely to zero in the presence of CO₂. Or it may be due partly to a small residual passive component of sodium flux.

There was no systematic effect of CO₂ on R_{∞} , indicating that the region of the skin responsible for this resistance is not associated with active transport.

Relation of Electrical Impedance to Structure. The series resistance, R_{∞} , averaging about 150 ohm-cm², is only a small fraction of the total low frequency impedance. Choline and isethionate ions can contribute to the current through this resistance, although not quite as readily as sodium and chloride ions. Thus, most likely R_{∞} is developed in rather loosely packed tissue, specifically the outer epithelium and the subepithelial connective tissue. The fluid between the electrodes and the skin is a part of this resistance, but contributes little because the product of the conductivity of the solution (about 87 ohm-cm for the normal solution) and the electrode spacing (0.2 to 0.3 cm) gives about 20 ohm-cm² as the maximum resistance of the solution alone. This tissue is not associated with active transport since R_{∞} is not altered by CO₂.

The conductance, g_p , is in parallel with the large "capacitance" and thus must be developed within a relatively thin tissue layer. The large low frequency impedance and the impermeability of the layer to choline and isethionate ions implies a continuous membrane or a closely packed cell layer. The response to CO₂ indicates a direct connection between g_p and active transport. Thus, the most likely location of

this element is a cell membrane of the germinative epithelial layer (or, perhaps, the epithelial basement membrane.)

Transport Kinetics. In planning these experiments, we hoped to elucidate the kinetics of the active transport system by evaluating the velocity of the reactions involved. However, the element exhibiting frequency dependence, the phase shift element, does not appear to be associated with active transport, while the parallel conductance, g_p , which does correlate with active sodium movement, is not a function of frequency, at least up to about 5 kc/second, the limit of validity of this equivalent circuit. Thus, the velocity of these reactions must be too rapid to lead to significant phase shifts in response to voltage alterations at these frequencies. The alternative, that the active transport pathway is separate from the AC conductance pathway and therefore is unaffected by the applied AC potential, appears unlikely in view of the relation between g_p and active transport.

SUMMARY AND CONCLUSIONS

1. The AC electrical impedance of frog skin in the range 1 to 5000 cycle/second, is described by equation (1). It can be represented by an equivalent circuit consisting of a series resistance, R_∞ , and a parallel combination of a conductance, g_p , and a phase shift element, Z' .

2. The phase shift element has an impedance angle of about 80° , current leading voltage; the equation for its impedance is $R_p(j\omega\tau)^{\alpha-1}$, $\alpha \approx 0.11$. The equivalent capacitance calculated from τg_p is $2.24 \mu\text{f}/\text{cm}^2$. The phase shift and the equivalent capacitance are independent of all experimental conditions employed here.

3. The parallel conductance, g_p , which is responsible for most of the low frequency impedance, is composed of two approximately equal conductances, one associated with sodium ion current (g_{Na}) and the other associated with chloride ion current (g_{Cl}). Both g_{Na} and g_{Cl} depend mainly on the composition of the solution perfusing the outside surface of the skin. The conductance g_{Cl} appears to be directly proportional to the outside concentration of chloride, while g_{Na} shows saturation at low outside concentrations of sodium. It is possible to greatly reduce g_{Na} , even in the presence of normal sodium concentration, when active transport is suppressed by CO_2 . Thus, little sodium can pass through the skin if it does not pass through in association with the active transport mechanism.

4. The series resistance, R_∞ , is most probably developed in the surface epithelium and the subepithelial connective tissue; the parallel components, g_p and the phase shift element, are probably located in the germinative epithelial layer or the basement membrane.

Supported in part by grants GM739 and HTA5147 from the United States Public Health Service. K. G. Kastella is a National Science Foundation Fellow.

Received for publication, November 16, 1964.

REFERENCES

- BROWN, A. C., 1962, Current and potential of frog skin *in vivo* and *in vitro*, *J. Cell. Comp. Physiol.*, **60**, 263.
- COLE, K. S., and CURTIS, H. J., 1936, Electrical impedance of nerve and muscle, *Cold Spring Harbor Symp. Quant. Biol.*, **4**, 73.
- FALK, G., and FATT, P., 1964, Linear electrical properties of striated muscle fibres observed with intracellular electrodes, *Proc. Royal Soc. London Series, B.*, **160**, 69.
- FATT, P., 1964, An analysis of the transverse electrical impedance of striated muscle, *Proc. Royal Soc. London Series, B.*, **159**, 606.
- KIRSCHNER, L. B., 1955, On the mechanism of active sodium transport across frog skin, *J. Cell. Comp. Physiol.*, **45**, 61.
- MOORE, W. J., 1955, *Physical Chemistry*, second edition, Englewood Cliffs, New Jersey, Prentice-Hall.
- RANCK, J. B., JR., 1963*a*, Specific impedance of rabbit cerebral cortex, *Exp. Neurol.*, **7**, 144.
- RANCK, J. B., JR., 1963*b*, Analysis of specific impedance of rabbit cerebral cortex, *Exp. Neurol.*, **7**, 153.
- SCHWAN, H. P., 1957, Electrical Properties of Tissue and Cell Suspensions. *in Advances in Biological and Medical Physics*, J. H. Lawrence and C. A. Tobias, editors, New York, Academic Press.
- SMYTH, C. P., 1955, *Dielectric Behavior and Structure*, New York, McGraw-Hill Book Company, Inc.
- SNELL, F. M., and LEEMAN, C. P., 1957, Temperature coefficients of the sodium transport system of isolated frog skin, *Biochim. et Biophysica Acta*, **25**, 311.
- USSING, H. H., 1960, The frog skin potential, *J. Gen. Physiol.*, **43**, (5), p. 2, 135.
- USSING, H. H., and ZERAHN, K., 1951, Active transport of sodium as the source of electric current in the short-circuit isolated frog skin. *Acta Physiol. Scand.*, **23**, 110.